**Rare Metal Materials and Engineering**
Volume 52, Issue 7, July 2023
Available online at www.rmme.ac.cn

Science Press

**Cite this article as**: Xu Yi, Zhang Bing, Yang Yan, et al. Microstructure Evolution and Mechanical Properties of GH4169 Alloy During Cold Rolling and Heat Treatment[J]. Rare Metal Materials and Engineering, 2023, 52(07): 2385-2395.

ARTICLE

# Microstructure Evolution and Mechanical Properties of GH4169 Alloy During Cold Rolling and Heat Treatment

**Xu Yi[1,2], Zhang Bing[1,2], Yang Yan[3], Chen Le[1,2], Zhao Tianli[1,2], Wang Qi[4], Zhang Zhijuan[1,2], Yang Ben[1,2], Zan Bin[3], Cai Jun[1,2], Wang Kuaishe[1,2]**

*[1] College of Metallurgical Engineering, Xi'an University of Architecture and Technology, Xi'an 710055, China; [2] National and Local Joint Engineering Research Center for Functional Materials Processing, Xi'an University of Architecture and Technology, Xi'an 710055, China; [3] State Key Laboratory of Nickel and Cobalt Resources Comprehensive Utilization, Jinchang 737100, China; [4] Jinchuan Group Nickel Alloy Co., Ltd, Jinchang 737100, China*

**Abstract:** The microstructure evolution and mechanical properties of GH4169 alloy during cold rolling and heat treatment were investigated by scanning electron microscope, electron backscatter diffraction, and transmission electron microscope. Results show that the grains are elongated into fibers with increasing the cold rolling deformation degree, and no $\delta$ phase can be observed in the microstructure. After heat treatment, the original deformed grains are replaced by small recrystallized grains, and the grain size is decreased with increasing the cold rolling deformation degree and decreasing the heat temperature. However, the mixed grain structure appears after cold rolling deformation of 50%. When the heat treatment temperature is 950 and 990 °C, the $\delta$ phase is precipitated in the matrix. The content of $\delta$ phase is increased with increasing the deformation degree and the morphology is changed from short rods into spherical shapes. When the deformation degree is 70%, the ultimate tensile strength (UTS) reaches 1484.27 MPa, which is 1.92 times higher than that of the cold rolled alloy (772.5 MPa). However, the elongation (EL) decreases to 8.93%, and it increases to 46.47% after heat treatment at 990 °C, which is 5.2 times higher than that of the cold-rolled alloy. The optimal combination of mechanical properties (UTS=943.59 MPa, EL=52.31%) can be achieved when the cold rolling deformation degree is 50% and the heat treatment temperature is 990 °C.

**Key words:** GH4169; cold rolling; heat treatment; $\delta$ phase; mechanical characteristics

GH4169 alloy is widely used in aerospace, nuclear energy, and oil and gas fields due to its excellent mechanical properties, weldability, good oxidation resistance, and corrosion resistance[1–4]. As a precipitation-strengthened superalloy, the excellent comprehensive properties are mainly attributed to the precipitated phase in GH4169 alloy. GH4169 alloy is basically composed of austenite $\gamma$ phase matrix, which includes the strengthening $\gamma''$ phase $Ni_3Nb$, auxiliary strengthening $\gamma'$ phase $Ni_3(Al, Ti)$, $\delta$ phase $Ni_3Nb$, and a small amount of carbide[5–9]. Among them, the $\delta$ phase acts as the equilibrium phase, which also significantly affects the mechanical properties of GH4169 alloy. Currently, it is reported that the $\delta$ phase usually has the following effects on the mechanical properties of GH4169 alloy. (1) The stress concentration will be generated around the needle-like $\delta$ phase, forming micropores or even interface separation and reducing the strength and fatigue properties of GH4169 alloy[10–11]. (2) The $\delta$ phase can reduce the yield strength and notch sensitivity of GH4169 alloy, but it can significantly increase the alloy plasticity[12–13]. (3) The fine diffused $\delta$ phase can pin the grain boundaries, inhibit the grain growth, and exert the fine grain strengthening effect[14–15]. The features of $\delta$ phase (morphology, content, and distribution) have important effects on the mechanical properties of alloys, thereby requiring further investigation.

The $\delta$ phase and microstructure are extremely sensitive to

Received date: March 02, 2023
Foundation item: Major Science and Technology Program of Gansu Province (20ZD7GC009); Scientific and Technological Innovation Team Project of Shaanxi Innovation Capability Support Plan, China (2022TD-30)
Corresponding author: Zhang Bing, Ph. D., Professor, College of Metallurgy Engineering; Xi'an University of Architecture and Technology, Xi'an 710055, P. R. China, E-mail: bingzhang1112@xauat.edu.cn

mechanical processing. The nucleation and growth of the $\delta$ phase are significantly influenced by the original organization and stress of base material (BM)[11,16]. Most researches focus on the optimization of the heat treatment scheme to achieve better $\delta$ phase regulation in GH4169 alloy, but the effect of processing technique is rarely reported[17–18]. In addition to the significant effect of precipitation on the properties of GH4169 alloy, the grain features, such as morphology and size, are also important to the alloy properties. Grain refinement can hardly be achieved by heat treatment. Normally, the grains can only be refined by recrystallization during the cold/hot working process[19–20]. Therefore, it is necessary to investigate the effects of different processing processes on the $\delta$ phase, grain characteristics, and mechanical properties of GH4169 alloy.

GH4169 alloy has large deformation resistance, because it is mainly formed by hot deformation, such as hot forging and hot rolling. The microstructure evolution during hot deformation and subsequent heat treatment processes have been extensively researched[21–23]. Wang et al[24] investigated the effect of hot compression deformation on the $\delta$ phase content and found that the content of $\delta$ phase is decreased with increasing the strain and increased with decreasing the strain rate during thermal deformation at 950 °C. Páramo-Kañetas et al[25] found that during thermal deformation and thermal annealing, small and dispersed $\delta$ phase can be obtained near the grain boundaries of GH4169 alloy, which is beneficial to homogenization and grain refinement. Compared with that of the hot-deformed alloys, the alloy microstructure can be easily controlled by cold deformation with high forming accuracy. However, the effects of cold deformation and subsequent heat treatment on the microstructure and mechanical properties of GH4169 alloy are barely investigated. Huang et al[26] obtained the thin plates of small-grained GH4169G alloy (ASTM13) by cold rolling and heat treatment. Xue et al[27] investigated the microstructure of alloys after different cold rolling deformation and subsequent heat treatments at 900 °C for 10 h. It is found that the cold rolling can increase the nucleation rate of $\delta$ phase and reduce the critical nucleation work during heat treatment, thereby promoting the precipitation of $\delta$ phase. Mei et al[28] investigated the effect of cold rolling on the phase precipitation of Inconel 718 alloy. It is reported that after isothermal aging at 950 °C for 6 h, the cold rolling can significantly accelerate the $\delta$ phase precipitation and modify the morphology of $\delta$ phase into spherical shape. Zhang et al[29] found that proper cold rolling can improve the resistance against crack propagation, and the spherical-like $\delta$ phase improves the mechanical characteristics at 650 °C. Clearly, the combination of cold deformation and heat treatment can regulate the microstructure and enhance the properties of GH4169 alloy.

In this research, the effects of cold rolling deformation and heat temperature on $\delta$ phase and grain characteristics of GH4169 alloy were investigated. The relationship between the $\delta$ phase and recrystallized grains was analyzed. The influence of microstructure on mechanical properties of GH4169 alloy was discussed.

## 1 Experiment

BM used in this research was hot-rolled GH4169 alloy plate with the dimension of 5.2 mm (thickness)×90 mm (width)× 140 mm (length). The chemical composition of GH4169 alloy is shown in Table 1.

Unidirectional multi-pass cold rolling was conducted on GH4169 alloy plate by a reversible two-roll mill with rolling deformation degree of 30%, 50%, and 70%. The specimens with deformation degree of 50% were heat-treated at 950, 990, 1030, and 1070 °C for 60 min under argon protection and then immediately quenched by water to room temperature to retain the high-temperature microstructure. In addition, the plates with deformation degree of 0%, 30%, 50%, and 70% were treated at 990 °C for 60 min to study the effects of deformation.

Microstructure was observed along the rolling direction (RD)-normal direction (ND) planes. After grinding, mechanical polishing, and chemical etching (10 mL $HNO_3$+30 mL $H_2O$+40 mL HCl+3.5 g $CuCl_2$), the specimens after cold rolling and heat treatment were observed by optical microscope (OM) and Gemini SEM 300 field emission scanning electron microscope (SEM). The volume fraction of $\delta$ phase was calculated through ImageJ software. The specimens for electron backscattered diffraction (EBSD) analysis were electropolished at room temperature with electrolyte (volume ratio of perchloric acid to alcohol=1:9), and then they were analyzed by SEM with scanning step size of 0.16 mm. The data were analyzed by Channel 5 software. In addition, the specimens for transmission electron microscope (TEM) analysis were ground to the ones with size of 40 – 50 μm, then twin-jet electropolished, and finally analyzed by FEI Talos F200X TEM.

To evaluate the mechanical properties of GH4169 alloy at different stages, the dog-bone-shaped tensile specimens of 20 mm (gauge length)×5 mm (width) were prepared along RD of GH4169 alloy sheet. Room-temperature tensile tests were conducted by the Instron 8801 electro-hydraulic servo fatigue test system at strain rate of $1.0\times10^{-3}$ $s^{-1}$. Three

**Table 1 Chemical composition of GH4169 alloy (wt%)**

| C | Cr | Ni | Co | Mo | Al | Nb |
|---|---|---|---|---|---|---|
| 0.02–0.06 | 17.00–21.00 | 50.00–55.00 | ≤1.00 | 2.80–3.30 | 0.30–0.70 | 5.00–5.50 |
| B | Mg | Mn | Si | p | S | Fe |
| ≤0.006 | ≤0.005 | ≤0.35 | ≤0.35 | ≤0.015 | ≤0.015 | Bal. |

specimens of each group were tested to evaluate their tensile properties. The fracture morphologies of the tensile specimens were observed by SEM coupled with energy dispersive spectrometer (EDS).

## 2 Results and Discussion

### 2.1 Microstructure evolution during cold rolling

Fig. 1 shows the microstructure of GH4169 alloy after different cold-rolling deformations. As shown in Fig. 1a, BM microstructure has uniform equiaxed grain organization with average grain size of 63.81 μm, and the twins exist in some grains. After cold rolling deformation, the original equiaxial grains elongate along RD, the twins narrow, and the bending deformation occurs in a certain direction (marked by yellow arrows in Fig. 1b–1d). When the deformation degree increases to 50%, a few local shear bands appear (marked by red arrows in Fig. 1c). When the deformation degree increases to 70%, the grains elongate into fibrous shape, and a lot of shear deformation bands, which are parallel to each other, appear inside the grains at an angle to RD (marked by the red arrows in Fig. 1d), which result from the heterogeneous stress transmitted by neighboring grains or the inherent instability of grains during plastic deformation. This phenomenon indicates that the material undergoes locally inhomogeneous deformation after cold rolling with deformation degree greater than 50%. As shown in Fig. 1e–1h, the carbides (marked by white arrows) are diffusely distributed in the alloy matrix, and several positions are identified by EDS analysis as NbC and TiN. *M*C carbide has a tight arrangement of atoms and strong bonding force[30]. Therefore, it is stable in heat treatment and cold rolling. However, the $\delta$ phase cannot be observed in the matrix after cold rolling, which indicates that only the grain morphology changes during the cold rolling process.

Fig. 2 shows the inverse pole figures (IPFs), grain boundary (GB) maps, and Kernel average misorientation (KAM) maps of GH4169 alloy after cold rolling with different deformation degrees. As shown in Fig. 2a, the colors of each grain in BM are different, but the colors inside the grain are consistent, indicating that the grain orientation is random and the orientation is uniform inside the grains. However, the grain color of the alloy specimens with deformation degree of 30%, 50%, and 70% is cluttered, indicating that there is no obvious preferred orientation. This is because each grain suffers different deformation degrees during plastic deformation. To coordinate the deformation, the slip deformation occurs in the grain to rotate the lattice, leading to the changes in orientation of different parts of grains, and thereby forming deformation bands. Similar analyses are also reported in Ref.[31].

According to GB maps in Fig. 2e–2h, the proportion of low angle grain boundaries (LAGBs) in the alloys after cold rolling with deformation degree of 30%, 50%, and 70% is 88.39%, 87.59%, and 82.28%, respectively, which is much higher than that in BM (2.19%). A large amount of LAGB formation can better ameliorate the plastic deformation between nearby grains. The increase in LAGBs may be caused by the dislocation movement and dislocation pile-up within the deformed grains[32]. This is consistent with the variation in KAM maps (Fig. 2i–2l): the geometrically necessary dislocation density of the specimens increases after cold deformation and it is relatively high at grain boundaries, twin boundaries, and deformation zones. However, with increasing the deformation degree of cold rolling, the proportion of LAGBs decreases. This is because the deformation heat and the stored distortion energy are increased with improving the deformation degree, which alleviates the dislocation plugging phenomenon. Some LAGBs continue to absorb dislocations and then are transformed into high angle grain boundaries (HAGBs), forming deformation-induced boundaries (marked by black arrows in Fig. 2f – 2g). In addition, partial dynamic recrystallization may occur around the deformed grains under large deformation, resulting in the decrease in dislocation density and the decrease in LAGB proportion. It is worth

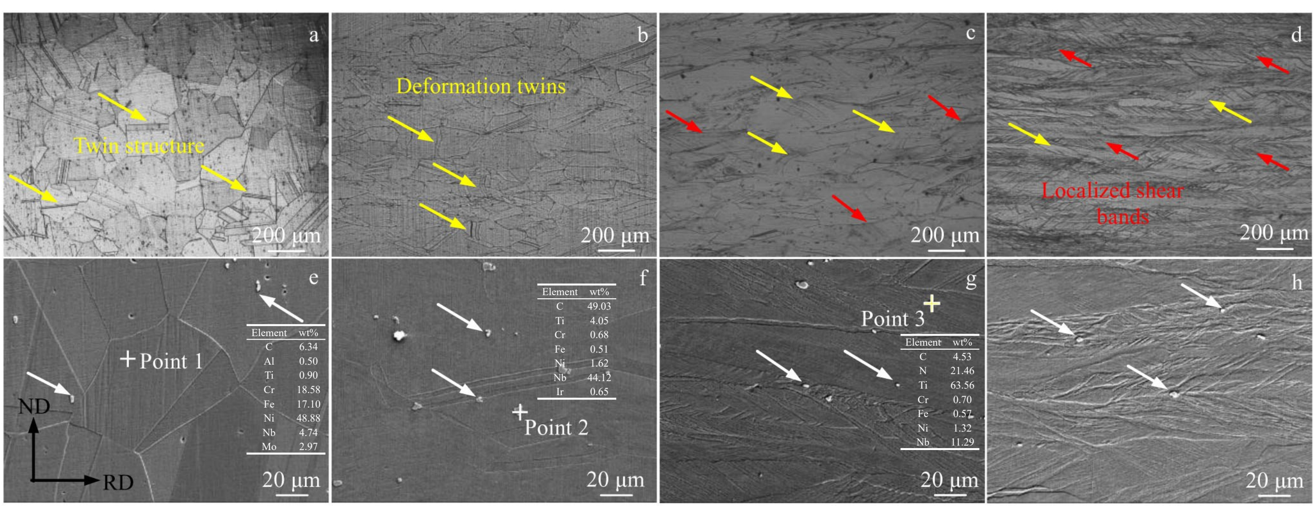


Fig.1 SEM microstructures and related EDS analysis results of GH4169 alloy after cold rolling of different deformation degrees: (a, e) 0%, (b, f) 30%, (c, g) 50%, (d, h) 70%

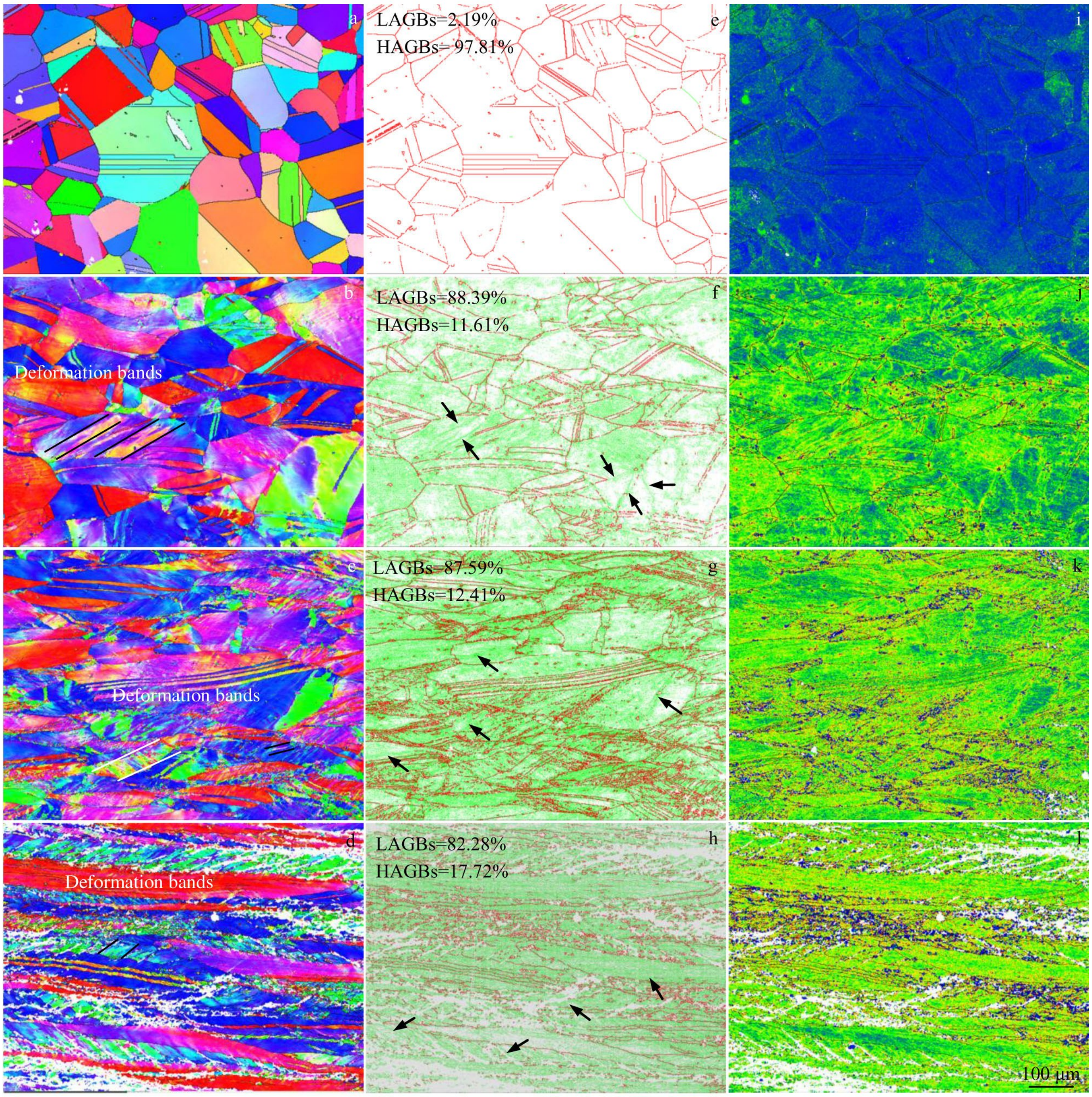


Fig.2 IPFs (a–d), GB maps (e–h), and KAM maps (i–l) of GH4169 alloys after cold rolling of different deformation degrees: (a, e, i) 0%, (b, f, j) 30%, (c, g, k) 50%, and (d, h, l) 70%

mentioning that the EBSD reheat is only 75% when the deformation degree is 70%, indicating the high lattice heterogeneity in the alloy, particularly around the grain boundaries and local shear zones. This phenomenon is caused by the high strain concentrations under cold deformation[33].

Fig. 3 shows TEM microstructures of cold-rolled GH4169 alloys with different deformation degrees. As shown in Fig.3a, BM specimen presents lower dislocations density and parallel dislocations along two directions which are perpendicular to each other, and therefore the cross slip can be observed. When the cold deformation degree increases to 30% and 50%, the dislocation density increases and the uneven localized dislocation entanglements are formed (Fig. 3c – 3d). In this case, the dislocation plane slip and dislocation multiplication are the primary deformation mechanism. As shown in Fig.3d, the severely deformed grains are distorted and broken when the deformation degree increases to 70%. Combined with the selected area electron diffraction (SAED) analysis, it is concluded that the high stress concentration and lattice distortion occur in the alloy after cold rolling with deformation degree of 70%. Liu et al[34] found that the significant grain breakage leads to lower EBSD reheat at deformation degree of 70%, which is similar to the results in this research.

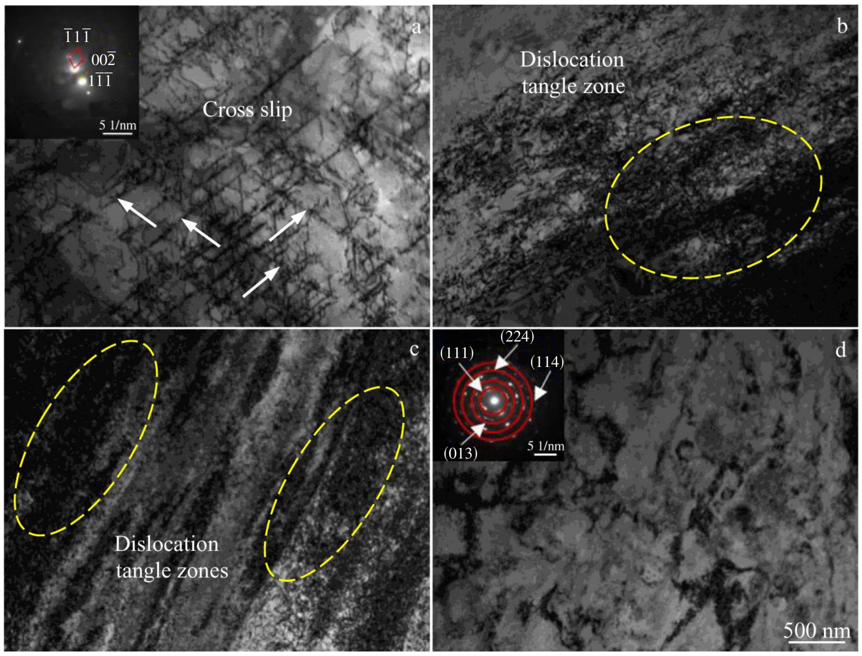


Fig.3 TEM microstructures and SAED patterns of GH4169 alloys after cold rolling of different deformation degrees: (a) 0%, (b) 30%, (c) 50%, and (d) 70%

**2.2 Microstructure evolution during heat treatment**

2.2.1 Effect of heat treatment temperature on microstructure

Fig. 4 shows SEM microstructures and EBSD maps of GH4169 alloys subjected to cold rolling with deformation degree of 50% and subsequent heat treatment at different temperatures. As shown in Fig. 4a and 4e, when the heat temperature is 950 °C, the matrix is mainly composed of short rod-like $\delta$ phase and a small amount of spherical $\delta$ phase. The volume fraction of $\delta$ phase ($V_\delta$) is 9.54% and the phase size is 2.15 μm. As shown in Fig. 4b and 4f, when the heat temperature rises to 990 ° C, $\delta$ phase dissolves and its morphology changes from short rod-like shape into spherical shape. $V_\delta$ decreases to 7.84%, and the phase size is reduced obviously to 0.57 μm. However, after heat treatment at 950 and 990 ° C, the $\delta$ phase is primarily distributed at grain boundaries and deformation zones, whereas other phases are sparsely distributed within the grains. This is because many defects exist in the grain boundaries and deformed strips. Thus, the non-equilibrium segregation of Nb leads to the preferential nucleation of $\delta$ phase, resulting in the non-uniform distribution of $\delta$ phase[35]. When the heat treatment temperature further rises to 1030 and 1070 ° C, $\delta$ phase gradually dissolves into the matrix, forming a supersaturated heat organization (Fig.4c–4d, 4g–4h).

As shown in Fig.4i–4l, the deformed grains are transformed into complete static recrystallization structures after heat treatment at temperatures below 990 °C. No obvious preferred orientation appears and the grains grow slowly. When the heat treatment temperature increases to above 1030 °C, the average grain size increases sharply from 8.49 μm to 25.57 μm. This is due to the large amount of $\delta$ phase precipitated in grain boundaries and grains after cold rolling (50%) and heat treatment below 990 °C. The $\delta$ phase provides nucleation sites for recrystallization, promotes recrystallization nucleation, hinders grain boundary migration, and inhibits the growth of recrystallized grains. Wang[36] and Chen[37] et al also obtained the similar results. In addition, a large number of nucleated recrystallization grains can also prevent the grain growth, thereby resulting in fine grains. It is worth mentioning that when the solution temperature is below 990 ° C, the inhomogeneous distribution of $\delta$ phase exists (Fig. 4a and 4b), which leads to the grains with non-uniform size, showing mixed grain structures. When the temperature is higher than 1030 ° C, the $\delta$ phase is completely dissolved, the average grain size increases rapidly under the high thermal energy, and the uniform recrystallization structure is obtained.

Fig. 5 shows TEM microstructures of GH4169 alloys subjected to cold rolling with deformation degree of 50% and subsequent heat treatment at 950 and 990 ° C. As shown in Fig. 5a, the long rod-like $\delta$ phase with size of about 2.64 μm can be observed, and the dislocations are packed around the $\delta$ phase. When the temperature increases to 990 ° C, the morphology of $\delta$ phase at the grain boundary becomes short rod-like and spherical shapes with the sizes of 1.47 and 0.65 μm, respectively, and the dislocation density around $\delta$ phase decreases (Fig. 5b). It is found that with increasing the temperature, the dislocation disappears and the dislocation slip occurs, promoting the dissolution of $\delta$ phase.

2.2.2 Effect of cold rolling deformation on microstructure

Fig.6 shows the microstructures of GH4169 alloy after cold rolling with different deformation degrees and subsequent heat treatment at 990 ° C. As shown in Fig. 6a, the $\delta$ phases with the short rod-like and spherical shapes are precipitated at

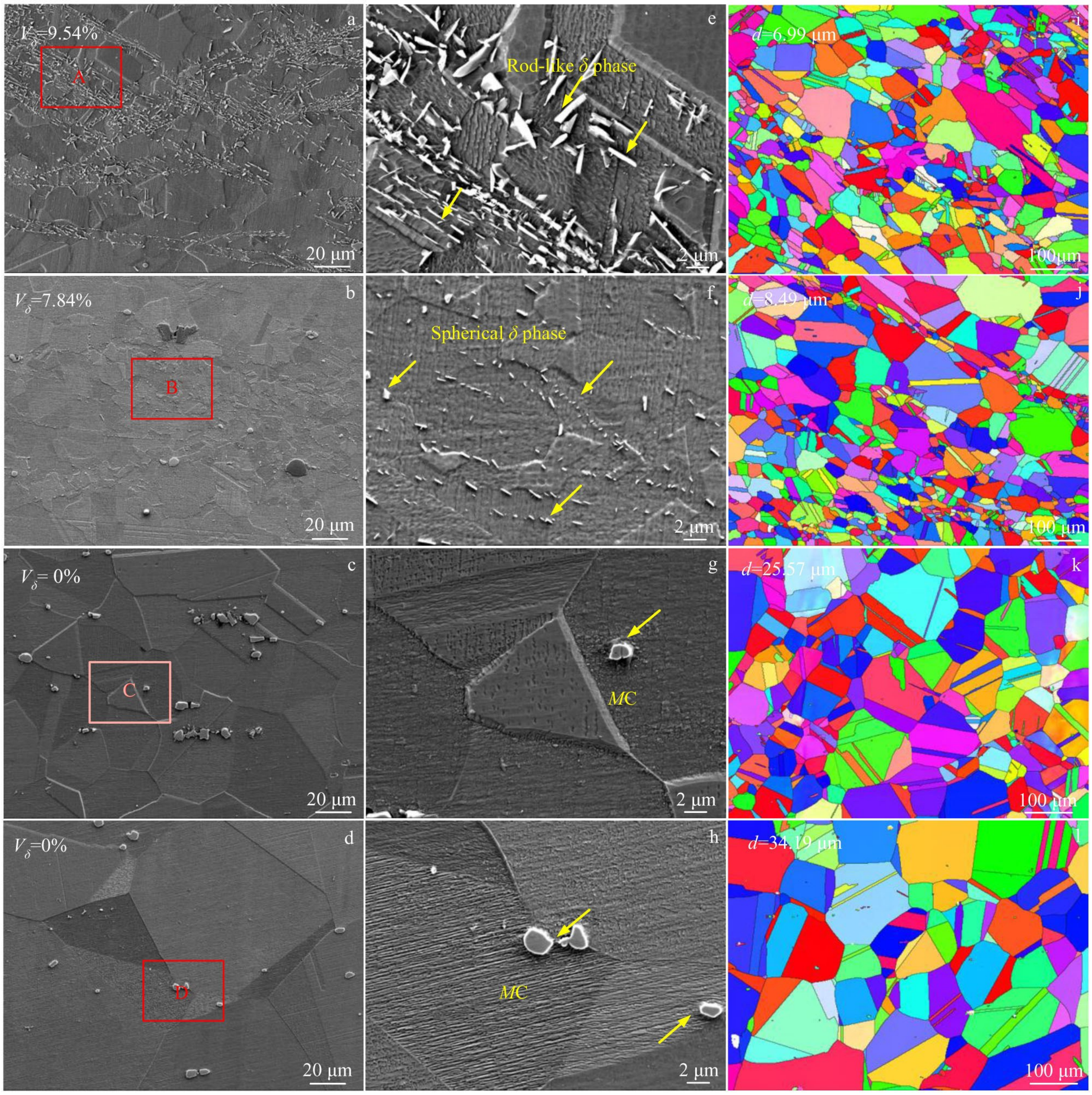


Fig.4 SEM microstructures (a–d) and IPFs (i–l) of GH4169 alloys subjected to cold rolling with deformation degree of 50% and subsequent heat treatment at different temperatures: (a, e, i) 950 °C, (b, f, j) 990 °C, (c, g, k) 1030 °C, and (d, h, l) 1070 °C; enlarged SEM microstructures of area A in Fig.4a (e), area B in Fig.4b (f), area C in Fig.4c (h), and area D in Fig.4d (h)

the grain boundaries in the undeformed specimen, the average size is 0.13 μm, and the content is 0.99%. As shown in Fig. 6b – 6d, the $\delta$ phase morphology is dominated by spherical shape with increasing the deformation degree. For the specimens after cold rolling deformation of 30%, 50%, and 70%, the $\delta$ phase content is 1.79%, 7.84%, and 9.63% with size of 0.82, 0.49, and 0.54 μm, respectively. It is obvious that the content of $\delta$ phase is increased and the phase size is decreased with increasing the deformation degree of cold rolling, indicating that the cold rolling deformation can induce $\delta$ phase precipitation and decrease the phase size. It can be seen that the $\delta$ phase is mainly distributed at the grain boundaries and shear deformation bands, but it barely exists in the grains. This is due to the large number of dislocations and defects formed in the shear deformation bands and grain boundaries during the cold rolling deformation. In addition, the nucleation conditions of the $\delta$ phase are improved. Thus, the $\delta$ phase is randomly distributed and becomes more significant with increasing the cold rolling deformation.

The grain size becomes smaller with increasing the deformation degree of cold rolling. The average grain size of specimens after cold rolling deformation of 30%, 50%, and 70% is 19.68, 8.46, and 4.52 μm, respectively, which is much

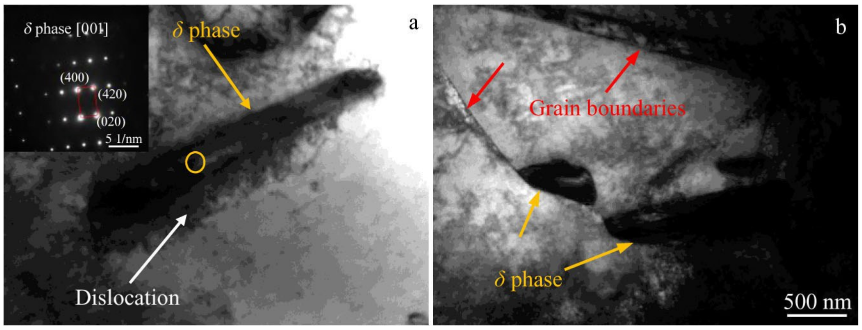


Fig.5 TEM microstructures and SAED pattern of $\delta$ phase for GH4169 alloys subjected to cold rolling with deformation degree of 50% and subsequent heat treatment at 950 °C (a) and 990 °C (b)

smaller than that of BM (85.65 μm). The grain size reduction can be attributed to the following two reasons. (1) The thermo-mechanical coupling of high temperature during heat treatment and the stored deformation energy under cold rolling deformation provides sufficient driving force for the nucleation of recrystallization. After cold rolling deformation, the energy storage of the alloy increases, and the driving force for the nucleation of recrystallization also increases during the heat treatment. Thus, the fine grains can be obtained. (2) $\delta$ phase promotes the recrystallization nucleation and inhibits the recrystallization growth. Therefore, the grain size becomes smaller with increasing the $\delta$ phase content. However, when the deformation degree of cold rolling is greater than 50%, the $\delta$ phase distribution is non-uniform, resulting in the formation of mixed microstructures containing a lot of small grains.

### 2.3 Mechanical properties

Fig. 7 shows the tensile properties of GH4169 alloys after cold rolling deformation and subsequent heat treatment. As shown in Fig.7a and 7d, the ultimate tensile strength (UTS) of BM is 772.5 MPa, and the elongation (EL) is 63.17%. After cold rolling, the alloy strength increases gradually, and the elongation gradually decreases. When the rolling reduction increases from 30% to 70%, UTS increases from 1083.94 MPa to 1484.27 MPa (1.92 times higher than that of BM), but EL decreases from 18.08% to 8.93%. This is due to the increase in dislocation density in the alloy during the cold rolling deformation (Fig. 3) and the work hardening effect. Meanwhile, the carbide hinders the dislocation slip, increases the alloy strength, and promotes the generation of deformation twins. Additionally, the shear bands also contribute to the increase in strength. Therefore, it can be concluded that the cold rolling with deformation degree of 50% exhibits the optimal comprehensive mechanical properties (UTS=1306.33 MPa, EL=10.80%).

As shown in Fig. 7b – 7c and 7e – 7f, the alloy strength decreases and the elongation increases after heat treatment. When the heat treatment temperature increases from 950 °C to 990 °C, the tensile strength and elongation of the alloy after cold rolling of deformation degree of 50% increase from 921.74 MPa and 45.44% to 943.59 MPa and 52.31%, respectively. When the heat treatment temperature further increases to 1070 °C, the tensile strength decreases to 768.56 MPa, but the elongation increases to 69.23% (Fig. 7b and 7e). The phenomenon that the alloy strength increases firstly and then decreases is attributed to the fact that the $\delta$ phase impedes the dislocation movement during tensile deformation, thereby enhancing the alloy strength. Compared with the short rod-like $\delta$ phase at 950 °C, the smaller spherical $\delta$ phase at 990 °C is beneficial to the uniform stress among grains, thus improving the alloy strength (Fig. 4). In addition, the grain refinement can effectively improve the strength and plasticity of metal materials. When the heat treatment temperature exceeds 990 °C, the $\delta$ phase in the alloy dissolves and the recrystallized grains grow, resulting in the reduction in alloy strength.

As shown in Fig.7c and 7f, compared with those of the cold-rolled GH4169 alloy, UTS of GH4169 alloy after cold rolling with deformation of 70% and subsequent heat treatment at 990 °C decreases to 949.47 MPa, whereas EL increases to 46.47%, which is 5.2 times higher than that of cold-rolled alloy. Additionally, with increasing the deformation degree, the strength of GH4169 alloys after cold rolling deformation and subsequent heat treatment at 990 °C is increased, whereas the elongation is decreased. This result is consistent with the variation trend of cold rolling state, but the magnitude of change extent reduces. This is because with increasing the cold rolling deformation, the grain size of the alloy is reduced, the $\delta$ phase content is increased, and the grain size is refined (Fig. 6). Fine grain strengthening and $\delta$ phase precipitation strengthening can maintain the plasticity and improve strength simultaneously. It can be seen that when the deformation degree of cold rolling is 50% and the heat treatment temperature is 990 °C, the tensile strength and plasticity are in great agreement: the tensile strength is 943.59 MPa and the elongation is 52.31%.

### 2.4 Fracture morphology

Fig. 8 shows fracture morphologies of GH4169 alloy after tensile tests. At room temperature, with increasing the deformation degree of cold rolling, the dimple morphology changes from large deep dimples into small shallow ones (Fig. 8a – 8d). After heat treatment, with increasing the heat

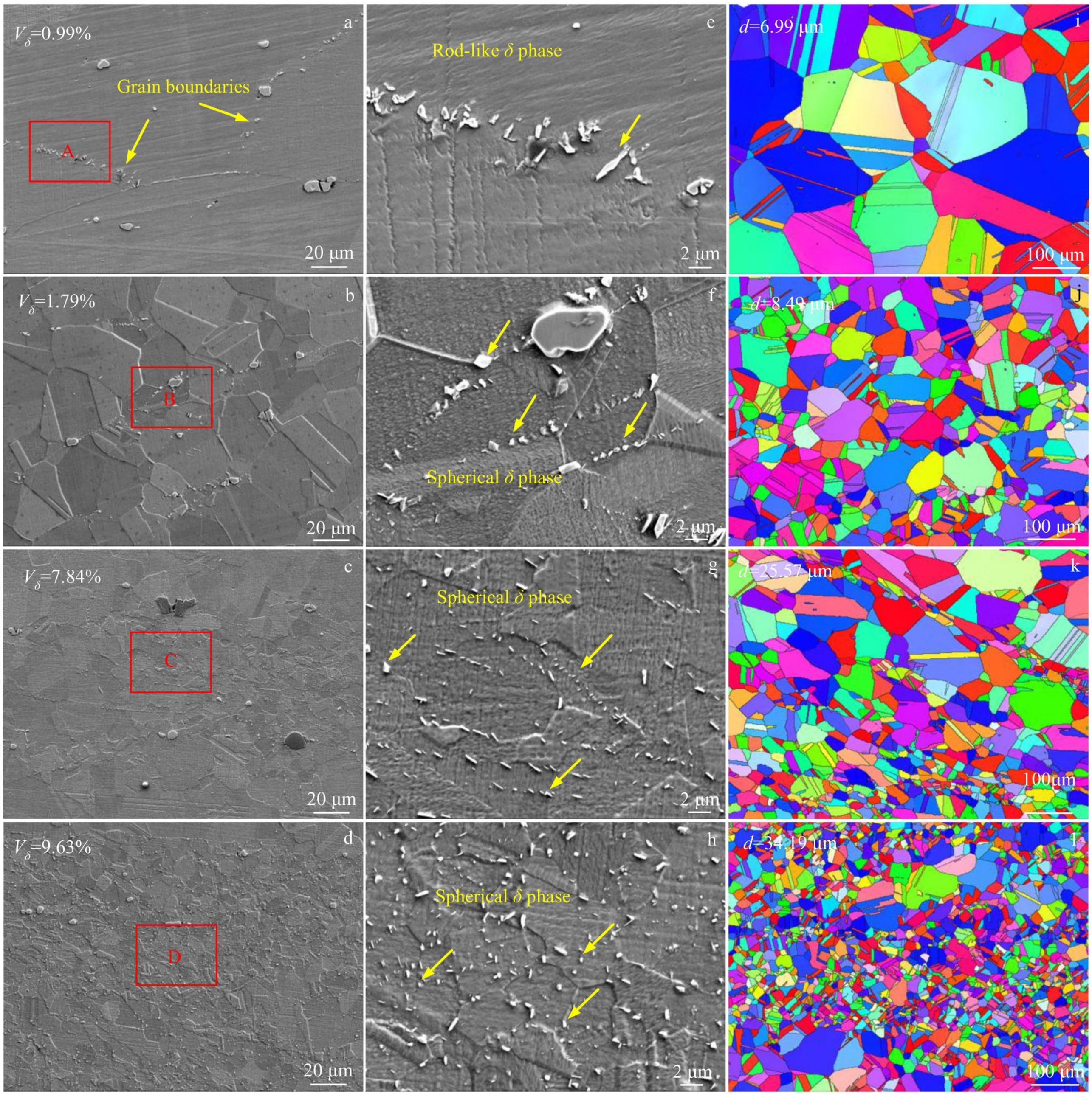


Fig.6 SEM microstructures (a–d) and IPFs (i–l) of GH4169 alloys subjected to cold rolling with deformation degree of 0% (a, e, i), 30% (b, f, j), 50% (c, g, k), and 70% (d, h, l) and subsequent heat treatment at 990 °C; enlarged SEM microstructures of area A in Fig.6a (e), area B in Fig.6b (f), area C in Fig.6c (h), and area D in Fig.6d (h)

treatment temperature, the dimple morphology changes from small shallow dimples into large deep ones (Fig.8e–8h). This phenomenon indicates that the alloy has better plasticity when the deformation is smaller or the heat treatment temperature is higher.

In addition, the particle phase can be found from the dimples in all GH4169 alloy specimens. According to EDS analysis results, the particle phases are NiC and TiN. During the tensile process, the plastic deformation of the carbide and matrix is not coordinated, which is prone to stress concentration and separation from the matrix, thus forming micropores. With the tensile test further proceeding, new micropores are formed and polymerized into microcracks until the fracture, resulting in round or elliptical dimples of different sizes. Therefore, the fracture pattern of GH4169 alloys is ductile fracture induced by microporous aggregation.

It is worth mentioning that although the morphology and quantity of $\delta$ phase change in the process, no necessary relationship is found between the $\delta$ phase and micropores in the fracture process. The $\delta$ phase induces slight dislocation diffusion, but it does not lead to the formation of significant pores, which is consistent with Ref.[38].

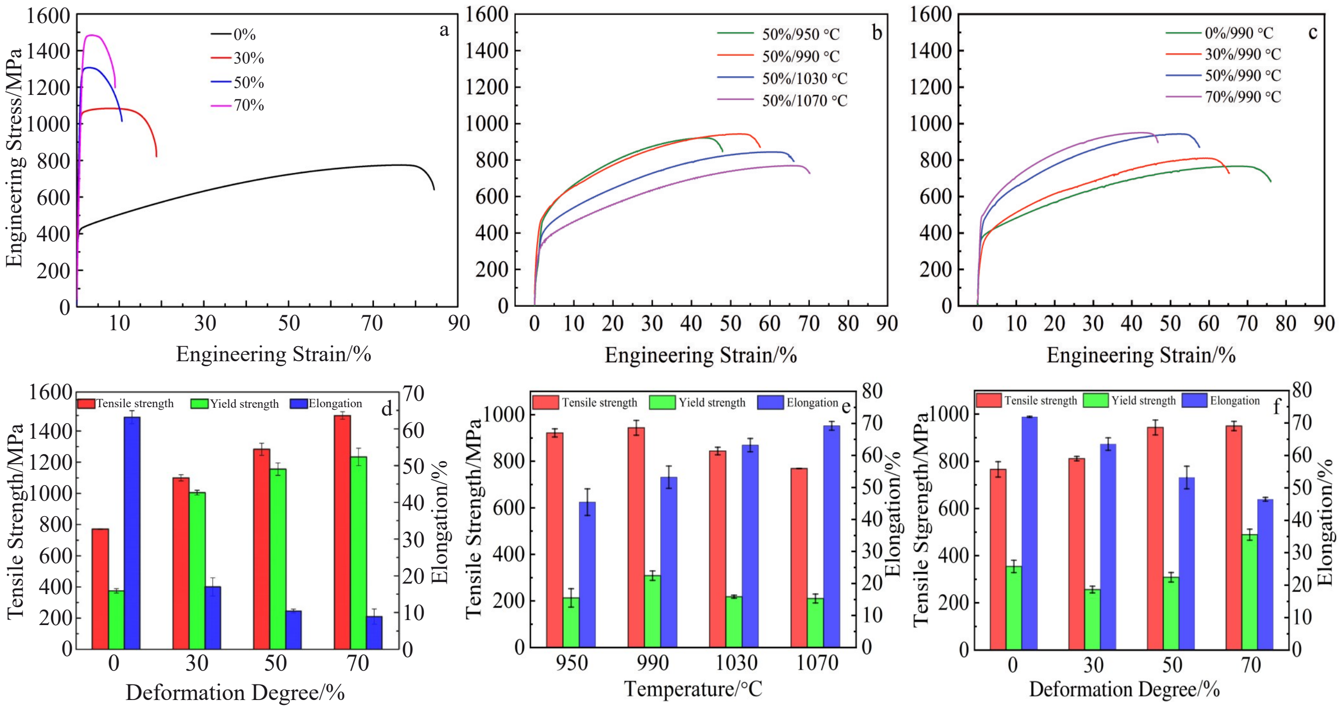


Fig.7 Engineering stress-engineering strain curves (a–c) and mechanical properties (d–f) of GH4169 alloys after different treatments: (a, d) cold rolling of different deformation degrees; (b, e) cold rolling of deformation degree of 50% and subsequent heat treatment at different temperatures; (c, f) cold rolling of different deformation degrees and subsequent heat treatment at 990 °C

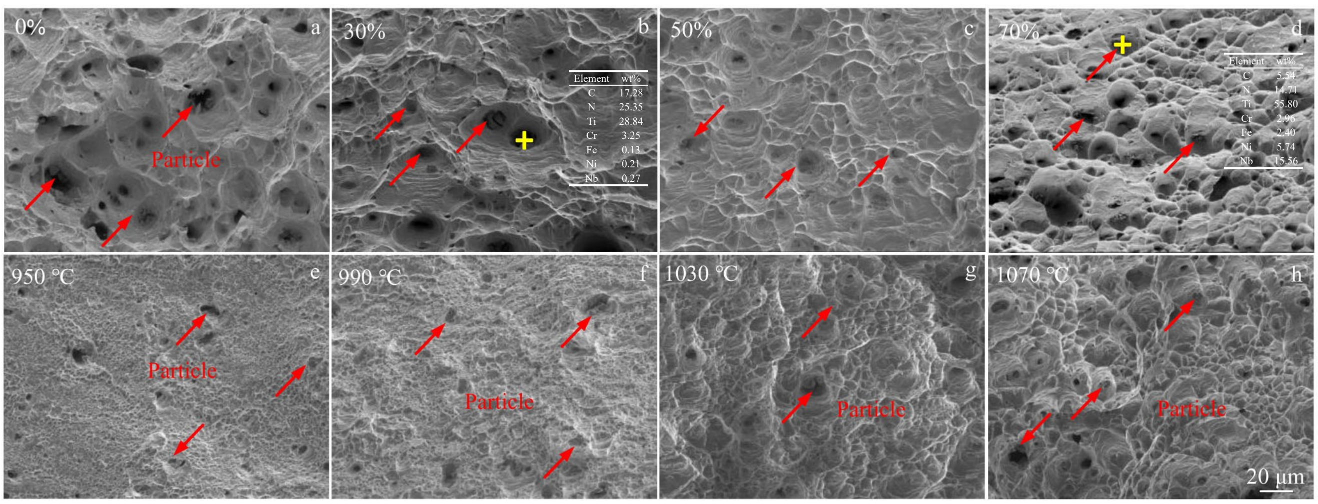


Fig.8 Fracture morphologies and EDS analysis results of the particle phases for GH4169 alloys after cold rolling of deformation degree of 0% (a), 30% (b), 50% (c), and 70% (d) and after cold rolling of deformation degree of 50% with subsequent heat treatment at 950 °C (e), 990 °C (f), 1030 °C (h), and 1070 °C (i)

## 3 Conclusions

1) The microstructure of cold-rolled GH4169 alloy consists of severely elongated and deformed grains, and some bending twins exist in the grains. When the deformation exceeds 50%, local shear deformation bands appear, indicating the non-uniform deformation. In addition, the $\gamma$ matrix of GH4169 alloy contains only NbC and TiN without the precipitation of $\delta$ phase.

2) After heat treatment, the original deformed grains are replaced by recrystallization grains. The average grain size is gradually increased with increasing the temperature, and it is decreased significantly with increasing the deformation degree of cold rolling. When the heat treatment temperature is below 990 °C, the short rods and spherical $\delta$ phase are precipitated in the matrix. With increasing the deformation degree, the $\delta$ phase content is increased and the phase size is decreased. $\delta$ phase has a significant effect on the grains. When $\delta$ phase

exists in the matrix, the grain size is smaller and the grain growth is inhibited. In addition, when the deformation degree exceeds 50% and the heat treatment temperature is below 990 °C, $\delta$ phase presents the inhomogeneous distribution, forming a mixed structure.

3) The strength of GH4169 alloy is increased gradually with increasing the cold rolling deformation. However, the strength of GH4169 alloy after cold rolling with deformation degree of 50% is firstly increased and then decreased with increasing the subsequent heat treatment temperature. The optimal comprehensive mechanical properties can be obtained when the deformation degree of cold rolling is 50% and the heat treatment temperature is 990 °C: the ultimate tensile strength is 943.59 MPa and the elongation is 52.31%.

4) The micropores introduced by *M*C carbides are the main reason for material failure. The fracture mode of GH4169 alloy is ductile fracture caused by the aggregation of micropores.

## References


1 Akca E, Gürsel A. *Periodicals of Engineering and Natural Sciences*[J], 2015, 3(1): 15

2 Demetriou V, Robson J D, Preuss M *et al*. *International Journal of Hydrogen Energy*[J], 2017, 42(37): 23 856

3 Chen Y T, Yeh A C, Li M Y *et al*. *Materials & Design*[J], 2017, 119: 235

4 Thellaputta G R, Chandra P S, Rao C S P *et al*. *Materials Today: Proceedings*[J], 2017, 4(2): 3712

5 Lan J, Huang H, Mao H J *et al*. *Materials Today Communications*[J], 2020, 24: 101 347

6 Rafiei M, Mirzadeh H, Malekan M *et al*. *Journal of Alloys and Compounds*[J], 2019, 795: 207

7 Zhao Xinbao, Gu Yuefeng, Lu Jintao *et al*. *Rare Metal Materials and Engineering*[J], 2015, 44(3): 768 (in Chinese)

8 Zhang, H J, Li C, Guo Q Y *et al*. *Scripta Materialia*[J], 2019, 164: 66

9 Li Yang, Wei Zhijian, Xu Pingwei *et al*. *Rare Metal Materials and Engineering*[J], 2020, 49(5): 1773 (in Chinese)

10 Wang Q, Ge S X, Wu D Y *et al*. *Materials Science and Engineering A*[J], 2022, 857: 143 859

11 Zhang S Y, Wang L L, Lin X *et al*. *Composites Part B: Engineering*[J], 2021, 224: 109 202

12 Shen Jialin, Wei Xianyi, Xu Pingwei *et al*. Rare Metal Materials and Engineering[J], 2019, 48(5): 1467 (in Chinese)

13 An X L, Zhang B, Chu C L *et al*. *Materials Science and Engineering A*[J], 2019, 744: 255

14 Huang R S, Sun Y A, Xing L L *et al*. *Materials Science and Engineering A*[J], 2020, 774: 138 913

15 Ran R, Wang Y, Zhang Y X *et al*. *Journal of Alloys and Compounds*[J], 2022, 927: 168 820

16 Da Cruz-Gallo F, De Azevedo L M B, Labre C *et al*. *Journal of Materials Research and Technology*[J], 2020, 9(2): 1801

17 Li F L, Bai Y R, Meng L C *et al*. *Materials Characterization*[J], 2020, 161: 110 175

18 Kim I S, Choi B G, Jung J E *et al*. *Materials Characterization*[J], 2020, 165: 110 378

19 An X L, Li Y, Ni S *et al*. *Materials Characterization*[J], 2020, 164: 110 360

20 Zhang J M, Gao Z Y, Zhuang J Y *et al*. *Journal of Materials Processing Technology*[J], 1999, 88(1–3): 244

21 He D G, Lin Y C, Jiang X Y *et al*. *Materials & Design*[J], 2018, 156: 262

22 Wang S, Wang Y, Zhang Y X *et al*. *Rare Metal Materials and Engineering*[J], 2022, 51(8): 2794

23 Chen M S, Zou Z H, Lin Y C *et al*. *Journal of Materials Science & Technology*[J], 2019, 35(7): 1403

24 Wang G Q, Li H B, Chen M S *et al*. *Materials Characterization*[J], 2021, 176: 111 130

25 Páramo-Kañetas P, Özturk U, Calvo J *et al*. *Journal of Materials Processing Technology*[J], 2018, 255: 204

26 Huang L J, Qi F, Sun W R *et al*. *Materials Science Forum*[J], 2014, 788: 43

27 Xue H, Zhao J Q, Liu Y K *et al*. *Transactions of Nonferrous Metals Society of China*[J], 2020, 30(12): 3287

28 Mei Y P, Liu Y C, Liu C X *et al*. *Journal of Alloys and Compounds*[J], 2015, 649: 949

29 Zhang H J, Li C, Guo Q Y *et al*. *Materials Science and Engineering A*[J], 2018, 722: 136

30 Liu Y Z, Jiang Y H, Zhou R *et al*. *Journal of Alloys and Compounds*[J], 2014, 582: 500

31 Yvell K, Grehk T M, Hedström P *et al*. *Materials Characterization*[J], 2018, 135: 228

32 Polkowska A, Lech S, Polkowski W. *Materials Science and Engineering A*[J], 2020, 787: 139 478

33 Peng M D, Shi J, Cui B *et al*. *Steel Research International*[J], 2017, 88(11): 1 700 069

34 Liu H L, Zhang M C, Xu M *et al*. *Materials Science and Engineering A*[J], 2021, 800: 140 280

35 Ran R, Wang Y, Zhang Y X *et al*. *Materials Science and Engineering A*[J], 2020, 793: 139 860

36 Wang Guanqiang, Chen Mingsong, Lin Yongcheng *et al*. *Science China Technological Sciences*[J], 2021, 64(8): 1741 (in Chinese)

37 Chen M S, Chen Q, Lou Y M *et al*. *Materials Science and Engineering A* [J], 2022, 831: 142 232

38 Yang X, Chen S N, Wang B X *et al*. *Journal of Materials Processing Technology*[J], 2022, 308: 117 696

# GH4169合金在冷轧和热处理过程中的组织演变和力学性能

徐　依[1,2]，张　兵[1,2]，杨　艳[3]，陈　乐[1,2]，赵田丽[1,2]，王　奇[4]，张志娟[1,2]，杨　奔[1,2]，昝　斌[3]，
蔡　军[1,2]，王快社[1,2]
(1. 西安建筑科技大学 冶金工程学院，陕西 西安 710055)
(2. 西安建筑科技大学 功能材料加工国家与地方联合工程研究中心，陕西 西安 710055)
(3. 中国镍钴资源综合利用国家重点实验室，甘肃 金昌 737100 )
(4. 金川集团镍合金有限公司，甘肃 金昌 737100)

**摘　要**：采用扫描电子显微镜、电子背散射衍射和透射电子显微镜研究了GH4169合金在冷轧和热处理过程中的组织演变和力学特征。结果表明，随着冷轧变形的增加，晶粒被拉长成纤维状，微观组织中未观察到$\delta$相。热处理后，原始变形晶粒被细小的再结晶晶粒取代，晶粒尺寸随着冷轧变形量的增加和热处理温度的降低而减小。但当变形量大于50%时，出现混合晶粒结构。热处理温度为950和990 ℃时，基体中存在$\delta$相析出。随变形量的增加，$\delta$相含量而增加，形态由短棒状变为球状。在冷轧状态下，当变形量为70%时，抗拉伸强度（UTS）达到1484.27 MPa，是冷轧态合金（772.5 MPa）的1.92倍，但延伸率（EL）降低到8.93%。然而经过990 ℃热处理后，延伸率提高到46.47%，是冷轧状态合金EL的5.2倍。冷轧变形量为50%、热处理温度为990 ℃时，获得了最佳的力学性能组合（UTS=943.59 MPa，EL=52.31%）。

**关键词**：GH4169；冷轧；热处理；$\delta$相；力学性能

作者简介：徐　依，女，1997年生，硕士，西安建筑科技大学冶金工程学院，陕西 西安 710055，E-mail：yi_xu228@163.com